IL-15 supports the generation of protective lung-resident memory CD4 T cells

Tara M. Strutt[1], **Kunal Dhume**[1], **Caroline M. Finn**[1], **Ji Hae Hwang**[1], **Catherine Castonguay**[2], **Susan L. Swain**[2], and **K. Kai McKinstry**[1,*]

[1]Division of Immunity and Pathogenesis, Burnett School of Biomedical Sciences, College of Medicine, University of Central Florida, Orlando, FL, USA

[2]Department of Pathology, University of Massachusetts Medical School, Worcester, MA, USA

Abstract

Tissue-resident memory T cells (T_{RM}) provide optimal defense at sites of infection, but signals regulating their development are unclear, especially for CD4 T cells. Here, we identify two distinct pathways that lead to the generation of CD4 T_{RM} in the lungs following influenza infection. The T_{RM} are transcriptionally distinct from conventional memory CD4 T cells, and share a gene signature with CD8 T_{RM}. The CD4 T_{RM} are superior cytokine producers compared to conventional memory cells, can protect otherwise naïve mice against a lethal influenza challenge, and display functional specialization by inducing enhanced inflammatory responses from dendritic cells compared to conventional memory cells. Finally, we demonstrate than an IL-2-dependent and a novel IL-2-independent but IL-15-dependent pathway support the generation of cohorts of lung T_{RM}.

Keywords

CD4 T cell; lung-resident T cell memory; influenza; interleukin-15

Introduction

Memory CD4 T cells provide strong protection against viruses through multiple pathways. They are especially important for clearing pathogens such as influenza A virus (IAV) against which neutralizing antibody alone cannot confer long-term immunity [1]. Several CD4 memory subsets have been described based on phenotypic, functional, and migratory

*Corresponding Author: K. Kai McKinstry, Division of Immunity and Pathogenesis, Burnett School of Biomedical Sciences, College of Medicine, University of Central Florida, 6900 Lake Nona Blvd., Orlando, FL, 32827, Phone: 407-266-7137, Fax: 407-266-7002, kai.mckinstry@ucf.edu.

Conflict of interest statement: The authors have no conflicts to declare.

Disclosure
The authors declare no competing financial interests.

properties [2], and optimal protection often involves multiple specialized populations acting in concert [3]. A challenge for developing T cell-based vaccines is thus identifying the kinds of memory cells needed for optimal clearance of individual pathogens and elucidating the signals required for the generation of each particular subset.

Tissue-resident memory T cells (T_{RM}) cells provide a first line of defense due to their location at sites of infection and display distinct functional attributes versus circulating memory subsets [2, 4–6]. CD8 T_{RM} formation is complex and appears to differ between tissue sites and the pathogen or priming model employed. The generation of CD8 T_{RM} primed by IAV, and in many other models, requires TGF-β-mediated upregulation of CD103 (a subunit of $\alpha_E\beta_7$ integrin) [7–13]. In contrast to CD8 T_{RM}, elevated CD103 expression is not usually observed on CD4 T_{RM} in either animal models or in humans [14, 15]. Thus, it is likely that distinct cytokine cues and perhaps other signals differentially regulate CD8 and CD4 T_{RM} generation and maintenance.

We recently found that IL-2 signals to effector CD4 T cells between 5–7 days post-infection (dpi) with IAV are crucial to direct memory development. The IL-2 signals enhance IL-7 receptor expression on CD4 T cells, thereby improving their access to IL-7 which is essential for the transition of effector cells into memory and for their survival thereafter. IL-2 also acts during this brief window of the CD4 T cell response to downregulate pro-apoptotic molecules, especially Bim, to promote short-term survival of effectors and to thus enable a greater cohort of cells for memory development [16, 17]. Almost all memory CD4 T cells primed by IAV in the spleen and draining lymph node (dLN) are dependent upon the receipt of IL-2 signals, as is a subset in the lung [16]. However, our studies also clearly indicate that a subset of memory cells in the lungs of IAV-primed mice, the primary site of infection, is IL-2-independent [16].

Here, we investigate the distinct subsets of IAV-primed memory CD4 T cells found in the lung, and the role of IL-2 and other cytokine signals in their generation. We find that T_{RM} comprise the majority of these memory cells, and surprisingly, that they include both an IL-2-dependent and an IL-2-independent subset. The IL-2-dependent and IL-2-independent CD4 T_{RM} share a surface phenotype that is distinct from conventional memory CD4 T cells present in the lung and spleen and express a distinct transcriptional profile including preferential expression of many of the genes found to differentiate CD8 T_{RM} from circulating memory CD8 T cells. The CD4 T_{RM} are characterized by enhanced cytokine production and an increased capacity to induce rapid inflammatory responses from dendritic cells (DC) as compared to conventional memory cells of the same specificity. Most importantly, CD4 T_{RM} are potent mediators of protection against IAV upon transfer to unprimed mice. Finally, we demonstrate that direct IL-15 signals to CD4 T cell effectors are required to generate the IL-2-independent CD4 T_{RM} subset, but that continued IL-15 is not required for its long-term maintenance. Our studies thus indicate that viral infection generates functionally specialized CD4 T_{RM} through distinct pathways, contributing to the heterogeneity of protective lung CD4 T cell memory.

Results

IAV primes IL-2-dependent and IL-2–independent lung-restricted CD4 T$_{RM}$

To investigate the role of IL-2 signaling in the generation of CD4 T$_{RM}$ we first transferred OT-II.Thy1.1 TcR Tg CD4 T cells to unprimed B6 mice and challenged with a low dose of A/PR8-OVA$_{II}$, recognized by the OT-II TcR [18]. We transferred 1×10^6 cells, a minimal number required to reliably track donor responses into the memory phase in this model of IAV infection. We used donor cells that had been primed in the presence of IL-2 *in vitro* prior to transfer in order to provide the requisite early-acting IL-2 signal needed to generate optimal CD4 T cell effector responses against IAV [16]. Groups of mice were treated with an isotype control Ab or with IL-2 neutralizing Abs from 1–7 days post-infection (dpi) to block conventional memory generation [16]. This IL-2 blocking regime faithfully replicates key aspects of the response of *Il2$^{-/-}$* CD4 T cells against IAV in the lung and secondary lymphoid organs [16]. In agreement with our previous findings in a similar adoptive transfer model in BALB/c hosts [16], peak effector expansion was equivalent in mice treated with IL-2 neutralizing or isotype Ab (not shown). However, IL-2 neutralization prevented virtually all donor cell recovery in the spleen and dLN by 28 dpi, but left a population of readily detectable IL-2-independent memory cells in the lungs (Fig 1a).

To determine if the IL-2-dependent and IL-2-independent memory cells detected in the lungs are T$_{RM}$ or a subset of circulating memory cells, we administered fluorescent anti-CD4 Ab intravenously to B6 hosts at 28 dpi and analyzed labeling of donor cells in the lung after 3–5 minutes. This technique can readily discriminate blood-borne cells present in the circulation, that become labeled with the intravenously administered Ab, versus those cells that are tissue-localized and thus protected from Ab labeling [19]. Roughly 80–90 percent of donor cells were not labeled (i.v.^{shielded}) in mice treated with isotype control Ab (Fig 1b), in agreement with previous studies demonstrating that the majority of lung memory CD4 T cells primed by IAV are not accessible to the vasculature [20]. Strikingly, all donor cells in mice treated with IL-2 neutralizing Ab are i.v.^{shielded} (Fig 1b). These i.v.^{shielded} donor cells in the lung fit criteria used to identify T$_{RM}$ [19]. To determine if the i.v.^{shielded} cells reside primarily in lung airways or the parenchyma, we separately analyzed donor cells recovered from the bronchial alveolar lavage (BAL) or the lung proper. Few i.v.^{shielded} donor cells were recovered by bronchiolar lavage (Fig 1c), indicating preferential parenchymal versus airway location of the i.v.^{shielded} memory cells in mice treated with either IL-2 neutralizing or control Ab.

Lung resident memory cells express a T$_{RM}$-associated phenotype

To define the relationship between the IL-2-dependent and IL-2-independent i.v.^{shielded} memory cells primed by IAV and T$_{RM}$ described in other models, we analyzed key surface markers CD103, CD69, and CD127. We also compared the phenotypes of i.v.^{sheilded} memory cells in the lungs to those of i.v.^{labeled} donor cells isolated from the lung. While IAV-primed CD8 T$_{RM}$ express high levels of CD103 which is known to be TGF-β-dependent[13, 21], all CD4 memory cells in the lung, whether i.v.^{labeled} or i.v.^{shielded} express low CD103 (Fig 1d and e). Furthermore, in separate experiments, we observed no change in donor cell recovery from lungs at 28 dpi in mice treated with either TGF-β neutralizing Ab

alone or with TGF-β neutralizing Ab in conjunction with IL-2 neutralizing Ab from 1–7 dpi (data not shown). These findings suggest that CD4 T_{RM} develop through a pathway distinct from that supporting IAV-specific $CD8^+$ $CD103^+$ TGF-β-dependent T_{RM}.

Most T_{RM} express high surface CD69, which promotes tissue retention through repression of the sphingosine 1 phosphate receptor [22–24]. The i.v.[shielded] donor cells in mice treated with IL-2 neutralizing or control Ab were uniformly CD69^{high} compared to i.v.[labeled] donors (Fig 1d and e). To determine if increased CD69 expression by the i.v.[shielded] memory cells is driven by recent TcR stimulation, we transferred OT-II cells from donor mice with GFP driven by the Nur77 protein locus (*Nr4a1*[eGFP]) that express GFP transiently after antigen stimulation [17, 25]. We compared GFP signal from i.v.[labeled] and i.v.[shielded] donor cells at 28 dpi to that from donor cells in unprimed hosts. All donor cells expressed low, uniform levels of GFP (Fig 1f), indicating that continuing cognate TcR stimulation is not responsible for maintaining the CD69 expression on either the IL-2-dependent or IL-2-dependent i.v.[shielded] cells, and arguing against a requirement for residual IAV antigen depots [26] in sustaining the $CD69^+$ memory cells.

We also analyzed IL-7 receptor expression (CD127), which is upregulated on CD4 T cells when they produce and respond to the autocrine IL-2 that facilitates effectors to transition to memory [16]. Intriguingly, the i.v.[shielded] memory cells in mice treated with either control or IL-2 neutralizing Abs expressed lower CD127 than did i.v.[labeled] memory cells (Fig 1d and e). This implies that the i.v.[shielded] subset may be less dependent on IL-7 survival signals compared to conventional memory CD4 T cells [27]. To test this, mice receiving donor cells and IL-2 neutralizing Ab were also treated with an IL-7 receptor blocking Ab starting at 14 dpi (when the virus is cleared) using a regime that in our previous studies reduced recovery of conventional CD4 memory cells primed by IAV by at least one log in the spleen and dLN, and to a lesser but significant degree in the lung [16]. IL-7 receptor blockade did not significantly reduce the recovery of the IL-2 independent lung memory cells (Fig 1g), which suggests that alternative survival factors regulate the maintenance of the i.v.[shielded] memory cells in the lung.

Finally, we sought to confirm that the i.v.[shielded] donor cells reside in the lung long-term rather than representing a transient subpopulation of circulating cells. We thus treated IAV-primed mice that had received donor cells with FTY720, which blocks egress from the lymph nodes and results in a dramatic loss of circulating T cells after short-term treatment [28]. Treatment for 5 days beginning at 23 dpi reduced the number of donor cells detected in the spleen by about 3-fold (Fig 1h), but had no impact on the number of donor cells detected in the lungs (Fig 1i), indicating that the i.v.[shielded] memory population in the lung is distinct from the circulating lymphocyte pool.

Together, these results support the hypothesis that after their initial priming, two distinct pathways, one IL-2-dependent and another that is IL-2-independent, support the generation of CD4 T_{RM} in the lung. The fact that T_{RM} generated in the presence and absence of IL-2 signaling share a common location and CD103^{low} CD69^{high} phenotype supports the hypothesis that alternate pathways exist produce closely related subsets of T_{RM} that are physiologically relevant.

A conserved T$_{RM}$ molecular signature

CD8 T$_{RM}$ are distinguished from circulating CD8 memory cells in mice and humans by a unique gene expression signature [7, 29, 30]. To determine if differences in transcriptional regulation similarly distinguish CD4 T$_{RM}$ and conventional memory cells primed by IAV, we performed whole genome microarray analysis comparing sort-purified donor T$_{RM}$ (i.v.^{shielded} CD69^{high}) from the lung mice against i.v.^{labeled} CD69^{low} donors obtained from the lung and spleen. At a threshold of > 1.5 and P value of 0.05, 79 transcripts representing 69 known genes were identified as being differentially expressed between the T$_{RM}$ and conventional memory cells (Fig 2a and Supp Table I). Differential surface expression of four of these genes, Slamf6, Tnfs11 (RankL), Klrg1, and Cdh1(CD324), was validated by flow cytometry (Fig 2b and c). The 69 genes clustered into 6 significant DAVID functional annotation clusters with the most enriched being 'cell adhesion' (Figure 2d and Supp Table I).

We next compared the 69 genes distinguishing lung CD4 T$_{RM}$ with the transcriptional signatures of CD103$^+$ CD8 T$_{RM}$ isolated from various mouse tissues in other studies, including lung CD103$^+$ T$_{RM}$ primed by IAV infection [7, 29]. Interestingly, nearly one quarter (23%; 16 of the 69 genes) of the genes identified as uniquely regulated in CD4 T$_{RM}$ overlap with the gene signature found to distinguish CD8 T$_{RM}$ from conventional memory CD8 T cells (Table I). Functional annotation clustering analysis of these 16 shared genes revealed a 12-fold enrichment in the 'GTPase regulator and activator' pathway (P-value 0.003) while those genes unique to CD4$^+$ T$_{RM}$ clustered in the 'cell adhesion' pathway (P-value 0.009). Remarkably, the CD4 T$_{RM}$ isolated from mice treated with IL-2 neutralizing Ab shared preferential expression of 15 of these 16 genes (Supplemental Table II). This analysis suggests that a key set of signature T$_{RM}$ genes, perhaps involved in maintenance or function, are shared between CD4 and CD8 T$_{RM}$ subsets, and between CD4 T$_{RM}$ generated by IL-2-dependent and IL-2-independent pathways, but that distinct cellular interactions in the lung may support the retention of CD4$^+$ versus CD8$^+$ T$_{RM}$.

CD4 T$_{RM}$ are functionally specialized and protective

The unique gene expression by CD4 T$_{RM}$ compared to conventional memory CD4 T cells suggests that the T$_{RM}$ may possess distinct functional qualities. To evaluate their respective functions, we first compared the cytokine production potential of the IL-2-dependent and IL-2-independent T$_{RM}$ to that of conventional i.v.^{labeled} memory cells. The T$_{RM}$ generated in the presence or absence of IL-2 contained similar frequencies of IFN-γ^+ and dual IFN-γ^+/IL-2$^+$ cells that were significantly greater than that of the conventional memory cells (Fig 3a, b, and c). This enhanced potential to produce IFN-γ suggests that the T$_{RM}$ may be better able to mediate protective responses against IAV, some of which depend on IFN-γ [31].

We have previously shown that memory CD4 T cells isolated from the spleen and draining lymph nodes of IAV-primed mice can protect otherwise naïve mice against a lethal dose of IAV upon adaptive transfer [31]. To test if the CD4 T$_{RM}$ are also protective, we isolated donor cells from lungs of IAV-primed mice that were treated with IL-2 neutralizing antibodies (in which all of the donor cells fit criteria of T$_{RM}$) and transferred them to new hosts. The 'take' of T$_{RM}$ was poor when the cells were transferred i.v. as compared to the recovery of an

equal number of i.v.[labeled] memory cells (Fig 3d), a result similar to that seen in studies of adoptive transfer of CD8 T_{RM} cells that reported limited survival of T_{RM} when introduced into the circulation [32]. Furthermore, those T_{RM} that could be re-isolated were largely confined to the lung versus the i.v.[labeled] donors that were found predominantly in the spleen (Fig 3e). We thus transferred the T_{RM} using the intranasal (i.n.) route. The 'take' of T_{RM} in the lung one day following i.n. transfer was about 3%, resulting in about 7.1×10^4 (+/-1.07×10^4) cells detected in the lungs after the transfer of 2.5×10^6 donor T_{RM}. No donor cells were detected in the spleen or dLN. This number of lung donor cells is in line with the physiological number of donor T_{RM} detected in IAV-primed mice at 28 dpi (see Figure 1). When the mice were challenged with a lethal dose of PR8-OVA$_{II}$, recipients of 4×10^6 or 2.5×10^6 T_{RM} were protected while recipients of 1×10^6 cells did not survive (Fig 3f). Protection mediated by the T_{RM} was associated with dramatically reduced viral titers versus those detected in control animals, that all succumbed to infection (Fig 3g left). Protection mediated by T_{RM} transfer was also antigen-dependent as the OVA-specific OT-II T_{RM} do not reduce viral titers in mice challenged with PR8 (lacking OVA$_{II}$ peptide expression) (Fig 3g right).

The earliest and perhaps most crucial function of CD4 T_{RM} in orchestrating protective responses is likely their ability to rapidly induce the production of inflammatory cytokines and chemokines in the tissue site. Indeed, very low numbers of memory CD4 T cells in the lung mediate control of IAV titers prior to the influx of other adaptive immune cells by jump-starting inflammatory responses from DC [33, 34]. To evaluate the role of T_{RM} in this function, we first compared the ability of sort-purified OT-II T_{RM} cells to activate bone marrow-derived DC pulsed with OVA$_{II}$ peptide *in vitro* versus an equal number of i.v.[labeled] OT-II memory cells isolated from the spleen. Both T_{RM} and splenic memory cells similarly activated DC to upregulate expression of CD40, CD86, and MHC-II by 40 hours of culture (Fig 4a). However, significantly higher levels of several cytokines and chemokines that we have previously correlated with protective inflammatory responses against IAV [33] were detected in co-cultures containing T_{RM} (Fig 4b).

We next asked if enhanced inflammatory responses from DC could be detected at early time points post-IAV challenge in the lungs of recipients of polyclonal CD4 T_{RM}. For these experiments, we sort-purified bulk i.v.[shielded] CD4 T cells from IAV-primed mice at 28 dpi and transferred 5×10^5 i.n. to new hosts that were then primed with IAV. We observed more IL-6$^+$ and IL-12$^+$ CD11c$^+$ cells at 4 dpi in recipients of T_{RM} (Fig 4c), as well as higher numbers of NK cells and neutrophils (Fig 4d and e). These results indicate the rapid initiation of local inflammatory responses by T_{RM} following IAV challenge involving multiple innate immune populations.

IL-15 is required to generate but not maintain IL-2-independent T_{RM}

Finally, we sought to determine if an alternative cytokine signal is required for the generation of CD4 T_{RM} through the IL-2-independent pathway. Given that IL-15 can support a degree of CD4 memory formation in some situations [35] we analyzed IL-15 expression following IAV challenge. We found that IL-15 protein in the lungs steadily increased during the first week of infection (Fig 5a), which is consistent with previous

studies analyzing gene expression [36]. In contrast, no IL-15 above background was detected in the serum (Fig 5a). The strong lung-restricted detection of IL-15 in response to IAV challenge suggests that it could be a central factor regulating $CD4^+$ T_{RM} generation.

To determine if IL-15 can support CD4 T_{RM} generation, we first treated mice receiving donor cells with IL-2 neutralizing Ab alone, thus restricting donor fate to T_{RM} (Fig 1), or with IL-2 neutralizing Ab in conjunction with a blocking Ab against CD122 (IL2/IL-15 receptor β chain) from 1–7 dpi. Blocking CD122 efficiently disrupts IL-15 signals *in vivo* [37–39], and because IL-2 is neutralized in these experiments, any impact of CD122 blockade can clearly be attributed to an impact on IL-15 and not IL-2 signaling. Efficient CD122 blockade was verified by FACS at 7 dpi on cells responding in the lungs (Fig 5b and c). The addition of anti-CD122 Ab did not reduce peak effector accumulation at 7 dpi (Fig 5d), consistent with reports that IL-15 does not affect CD4 T cell expansion during IAV challenge [40]. Strikingly, in mice treated with CD122 blocking and IL-2 neutralizing Abs, virtually no donor cells could be recovered at 28 dpi (Fig 5d), suggesting that the IL-2-independent T_{RM} pathway requires IL-15. To confirm this finding, and to rule out a depleting effect of the CD122 blocking antibody, we transferred OT-II cells to WT or $Il15^{-/-}$ B6 mice, challenged with IAV, and treated all hosts with IL-2 neutralizing Ab from 1–7 dpi. No differences in peak donor expansion were seen at 7 dpi in WT or $Il15^{-/-}$ hosts, but donor cells were virtually absent in $Il15^{-/-}$ hosts at 28 dpi, while T_{RM} were readily detected in WT hosts (Fig 5e). Together, these results demonstrate the generation of a CD4 T_{RM} subset in the lung through an IL-2-independent pathway that requires critical IL-15 signals during the first week of infection.

We next asked if the IL-15 signals needed to generate the CD4 T_{RM} must be delivered through trans-presentation, or if the CD4 T cells themselves need to express IL-15rα in order to mediate direct IL-15 signaling. To test this, we used WT ($CD90.1^+$/$CD90.2^+$) and conditional $IL15ra^{-/-}$ ($CD90.1^+$) OT-II cells transferred to the same or seperate WT ($CD45.1^+$) mice that were challenged with IAV and treated to block IL-2 from 1–7 dpi. Whether co-transferred or transferred to different hosts, the number of WT and $IL15ra^{-/-}$ donors was similar at 7 dpi, but at 28 dpi WT cells significantly outnumbered the $IL15ra^{-/-}$ donors (Fig 5f–h). This implies that effector cells require direct IL-15 signals within the first week of IAV infection to generate an IL-2-independent subset of CD4 T_{RM}.

Finally, we sought to determine if, in addition to being required for the initial generation of the T_{RM}, IL-15 was also required for the long-term maintenance of this subset. We thus transferred donor cells to mice that were challenged with IAV and treated with IL-2 neutralizing Ab from 1–7 dpi. Beginning on day 14 post-infection, coinciding with viral clearance in this model, mice were treated with CD122 blocking Ab or an isotype control every second day up to 28 dpi and the presence of donor T_{RM} analyzed on 30 dpi. While treatment with CD122 blocking Ab dramatically reduced the number of NK cells detected in the spleen (Fig 5i), a population known to be dependent on IL-15 for maintenance [41], the number of donor T_{RM} was equivalent in mice treated with control versus CD122 blocking antibody (Fig 5j). These results indicate that while IL-15 signals received within the first week of infection support the development of lung CD4 T_{RM}, continuous IL-15 signals are not required for the survival of this subset. This requirement for IL-15 during the first week

of infection is similar to the requirement for IL-2 during the first week of infection to form the IL-2-dependent T_{RM} subset, and supports the concept that these are alternate but parallel pathways.

Discussion

We previously found that autocrine IL-2 signaling of CD4 T cells, that is induced by cognate antigen recognition, is needed during the effector stage of IAV infection to generate virtually all memory cells present in secondary lymphoid organs. The IL-2 prevents acute death of effector cells during the contraction phase, and enhances their fitness to access IL-7 by upregulating sustained CD127 expression [16, 17]. Here, we show that IL-2 signals also support the generation of a subset of CD4 T_{RM} in the lung, which is consistent with findings of IL-2-dependent lung T_{RM} in an asthma model [42]. However, we also describe a novel IL-2-independent pathway in which direct IL-15 signals received by CD4 effector cells supports the generation of a separate but similar cohort of long-lived, highly functional and protective CD4 T_{RM} in the lung. As IL-2 and IL-15 both signal through the same CD122 receptor and downstream adaptor molecules, some of their respective impacts in promoting CD4$^+$ memory formation are likely similar. For example, like IL-2, IL-15 can mediate acute anti-apoptotic effects in activated CD4 T cells *in vitro* [43]. However, treatment with sub-saturating levels of IL-2 and IL-15 drives unique gene expression in T cells [44]. This suggests that key elements of the IL-15-dependent program promoting CD4 T_{RM} are likely distinct from the IL-2-dependent pathway, a hypothesis supported by the IL-7-independent survival of the IL-2-independent CD4 T_{RM}.

The remarkable degree of overlap in gene expression patterns distinguishing CD4 T_{RM} in this study and CD8$^+$ T_{RM} in other studies including those induced by similar IAV infection [7, 29] is notable. This suggests that a conserved molecular program supports the maintenance and function of all T_{RM} (CD4 and CD8) in non-lymphoid tissues. The prominence of genes differentially expressed by both CD4$^+$ and CD8$^+$ T_{RM} associated with GTPase activity suggests a central role for these proteins in T_{RM} homeostasis, possibly through regulating cell shape as indicated by studies of skin CD8 T_{RM} [45, 46]. On the other hand, that the genes we identified as uniquely expressed by lung CD4$^+$ T_{RM} were most enriched in cell adhesion pathways supports the hypothesis that different T_{RM} subsets (i.e. CD4$^+$ and CD8$^+$) within the same tissue may employ distinct mechanisms for local retention, perhaps indicating their residence in unique microenvironments. Recently, Hombrink et al. have demonstrated remarkable conservation of gene expression between lung-resident CD8 T_{RM} in mice and humans [47]. Further studies are required to determine to what extent the CD4 T_{RM}-specific gene expression patterns identified here translate into lung-resident human CD4 memory cells.

We found that the CD4 T_{RM} mediate robust protection against lethal IAV infection when transferred back to the lung. T_{RM}-mediated protection correlated with accelerated inflammatory responses in the lung marked by increased production of cytokines from dendritic cells and elevated numbers of innate cells. In previous studies this 'jump-start' of innate immunity by memory CD4 T cells correlated with early viral control [33, 34] and we also saw impressive reduction of viral titers in recipients of CD4 T_{RM}. The rapid induction

of inflammation likely also facilitates optimal CD8 T cell trafficking by establishing early chemokine gradients [48], and may help the response of other CD4 T cell specificities during heterosubtypic challenge [49]. Indeed, we found elevated levels of several chemokines in co-cultures of dendritic cells and T_{RM} compared to co-cultures with conventional memory cells. While all of these are factors are known to be produced by dendritic cells, further studies are required to determine if the T_{RM} are also capable of specialized production of distinct chemokine signals. Our analysis suggests that the ability of CD4 T_{RM} to induce enhanced inflammatory responses may be related to their expression of surface molecules known to impact APC function. For example, we found that Slamf6, which can interfere with T cell adhesion to DC [50], to be expressed at lower levels by T_{RM} than by conventional memory cells, and RANKL (TRANCE, TNFSF11), which can deliver an adjuvant-like signal to DC [51, 52], to be expressed at higher levels by T_{RM}. It is important to point out that only minor differences in surface expression of RANKL, CDH1, and KLRG1, which may nevertheless be biologically significant, distinguish T_{RM} and conventional memory cells. As such, these markers are not as suitable for distinguishing CD4 T_{RM} and other memory subsets as are levels of CD127 and CD69. Further studies are needed to investigate the relative importance of these and other distinguishing attributes of T_{RM} in contributing to their local retention, survival, and protective function.

IL-15 has been proposed to act as a local 'alarm' in tissues that promotes maximal Th1 and CD8 T cell responses needed to clear viral pathogens [53]. Our findings provide support that this 'alarm' can also act as a potent signal to induce long-lived CD4 T_{RM}. Although it is not clear from these studies that IL-15-production is strictly limited to the lungs, the lung-restricted detection of IL-15 following IAV infection supports the concept that T_{RM} generation is regulated through factors induced by infection at tissue sites. This is in sharp contrast to the CD4 T cell-intrinsic autocrine IL-2 signals that are absolutely required to promote conventional memory CD4 T cells primed by IAV [16, 17], and that also support a cohort of IAV-primed CD4 T_{RM}. While our studies show near identical phenotype and function of the IL-2- and IL-15-dependent T_{RM}, further work is required to determine whether these subsets play distinct or overlapping roles in protective immunity upon reinfection. A recent study employing IL-15-adjuvanted vaccinia-based IAV vaccination found that memory CD4^{+}, but not CD8^{+}, T cells played a predominant role in the protection generated [54]. Although T_{RM} subsets were not assessed, the authors found CD4 T cell responses in the lung were enhanced to a greater extent by IL-15 than those detected systemically [54]. This suggests that the incorporation of IL-15 into vaccination formulations, or strategies that lead to its local production, might boost the generation of protective, functionally specialized CD4 T_{RM} in the lung, and perhaps other tissues.

Methods

Mice

C57BL/6 (Taconic or Jackson Laboratories), B6.CD45.1 (Jackson), and *Il15*$^{-/-}$ mice on a C57BL/6 background (Taconic) mice were at least 8 weeks old at the time of infection. Donor CD4$^+$ T cells were obtained from 5–8 week old OT-II.Thy1.1 mice that express a TcR recognizing aa 323-339 (ISQAVHAAHAEINEAGR) of chicken ovalbumin (OVA). OT-

II.Thy1.1 mice, originally from Jackson Laboratories, were bred at the University of Massachusetts Medical School or at the University of Central Florida. *Nr4a1*[eGFP] expressing mice (Nur77 reporter mice) were originally obtained from Jackson Laboratories and used to breed *Nr4a1*[eGFP] OT-II donor mice. *Il15ra*[fl] mice, possessing loxP sites flanking exons 2–3 of the IL-15 receptor α chain (CD122) were obtained from Jackson Laboratories and bred to OT-II mice expressing Cre recombinase to generate conditional *Il15ra*^{−/−} OT-II mice. All experimental animal procedures were conducted in accordance with University of Massachusetts Medical School's and University of Central Florida's Animal Care and Use Committee guidelines.

CD4 T cell isolation and cell transfer

Naïve $CD4^+$ T cells from OT-II mice were obtained from pooled spleen and lymph nodes. Single cell suspensions were passed over nylon wool, followed by percoll gradient separation and positive MACS selection using CD4 microbeads (Miltenyi). Resulting cells were routinely >97% TCR^+ and expressed a characteristic naive phenotype (small size, $CD62L^{hi}$, $CD44^{lo}$ and $CD25^{lo}$). CD4 T cells were cultured under Th1-polarizing conditions including exogenous IL-2 as previously described [16]. The resulting effector cells were thoroughly washed and rested for at least 3 days in media free of antigen (Ag) from which live cells were purified by lympholyte separation (Cederlane). The resting, IL-2-primed donor cells were adoptively transferred to unprimed mice in 200 μl PBS by i.v. injection.

Donor CD4 T cells expressing CD90.1 were re-isolated from the lungs of IAV-primed CD90.2 B6 mice by first digesting and homogenizing lungs using GentleMACS (Miltenyi) followed by positive selection using MACS for CD90.1. The purity of donor cells was confirmed by FACS and 1-4×10^6 cells transferred i.n. to unprimed B6 hosts. In other experiments, $CD4^+$ i.v.[shielded] cells were obtained from lungs of donor B6 mice by cell-sorting followed by i.n. transfer of 5×10^5 cells to unprimed recipients.

Viral infection and in vivo treatments

A/PR8 and A/PR8-OVA$_{II}$ (H1N1) (kindly provided by P. Doherty) was grown in the allantoic cavity of embryonated hen eggs and characterized at the Trudeau Institute. Mice were infected intranasally under light isoflurane anesthesia (Webster Veterinary Supply) with a sublethal (0.1 LD$_{50}$) dose in 50 μl PBS. Mice received adoptively transferred T cells in 200 μL of serum-free media via intravenous or retro orbital injection and were infected on the same day.

In some experiments mice were treated with 250 μg per day of the anti-IL-2 Abs S4B6 and JES6-1A12 (Rat IgG2a) from 1–7 dpi, or with appropriate isotype control Ab (all from BioXcell). Some mice receiving anti-IL-2 Ab treatment were also given 250 μg of anti-CD122 Ab clone TM-β1 or isotype control (Rat IgG2b) from 1–7 dpi or an isotype control (Bioxcell). In other experiments mice were treated with an IL-7 receptor blocking antibody clone A7R34 (Bioxcell). All Ab was administered by intraperitoneal injection in 200 μL of PBS.

In some experiments IAV-primed mice were treated for 5 consecutive days with 2.5mg/kg of FTY720 (Cayman Chemical) dissolved in water by i.p. injection.

In vivo fluorescent Ab labeling, tissue preparation, and cell isolation

Anesthetized mice were injected i.v. with 3 μg of APC-labeled anti-CD4 Ab in 100 μL of PBS and euthanized 3–4 minutes later by cervical dislocation followed by exsanguination by perforation of the abdominal aorta. Lungs were perfused by injecting 10 ml of PBS in the left ventricle of the heart. Lungs, spleen, and draining mediastinal lymph node (dLN) were prepared into single cell suspensions by mechanical disruption of organs and passage through a nylon membrane, or by enzymatic digestion using GentleMACS (Miltenyi). In some experiments, donor cells from the lung or spleen were isolated using cell sorting based on expression of Thy1.1, CD69, and the i.v. administered APC-labeled anti-CD4 Ab.

Flow cytometry and intracellular cytokine staining

Flow cytometry was performed using fluorochrome-labeled Abs for surface staining anti-CD90.1 (OX-7), anti-CD90.2 (53-2.1), anti-CD4 (RM4.5), anti-CD69 (H12F3), anti-CD127 (A7R34), anti-CD122 (TM-β1), anti-CD103 (B-Ly7), anti-KLRG1 (2F1), anti-CDH1 (DECMA-1), anti-SLAMF6 (13G3-19D), anti-RANKL (IK22/5), anti-CD40 (1C10), anti-CD86 (GL1), anti-MHC-II (M5/114.15.2), anti-CD11c (HL3), anti-NK1.1 (PK136), anti-CD11b (M1/70), and anti-CD3 (17A2) (BD Biosciences, eBioscience, or BioLegend). Intracellular cytokine staining was performed by stimulating cells for 16 h with OVA$_{II}$ peptide-pulsed APC. After 2h, 10 μg/ml Brefeldin A (Sigma) was added and after a further 2 h, the cells were surface stained and fixed for 20 min in 4% paraformaldehyde. Intracellular staining was performed by permeabilizing the cells for 10 min in 0.1% saponin before staining for cytokine by the addition of anti-IFN-γ (XMG1.2), anti-IL-2 (JES-5H4), anti-IL-6 (MP5-20F3), anti-IL-10 (JES-16E3), anti-IL-12 (C17.8), and anti-IL-17 (eBio17B7) fluorescently labeled Abs. Analysis was performed using LSRII or Canto II instruments (BD Biosciences) and FlowJo (Tree Star) analysis software.

T cell and Dendritic cell co-culture and detection of cytokines and chemokines

Sort-purified OT-II memory cells from the lung (CD69^{+} i.v.^{shielded}) or spleen (CD69^{low} i.v.^{labeled}) 0.5×10^5/well, were co-cultured *in vitro* in Costar 24 well plates (Corning) in the absence or presence of OVA$_{II}$ peptide with 1×10^5 syngeneic bone marrow-derived dendritic cells (DC) prepared as previously described [16]. Levels of cytokines and chemokines in triplicate culture supernatants were determined using a mouse multi-plex luminex kit (Millipore) read on a Luminex 200 reader (Luminex Corp). Luminex analysis was similarly used to detect IL-15 protein from lung homogenates and serum samples.

Microarray analysis

Prior to harvest, mice receiving donor cells and IAV challenge 28 days prior were administered fluorescently-labeled anti-CD4 intravenously and spleens and lungs harvested 3–5 minutes later. Donor cells were isolated by first enzymatically digesting the tissues (GentleMACS) followed by cell sorting based on Thy expression (gating on donor Thy marker) and CD69 (used as a confirmatory marker for T$_{RM}$ in the lung).

Total mRNA was isolated (Qiagen) and amplified (Ambion) from sort purified populations of OT-II memory cells isolated from the lungs or spleens of IAV-primed mice at 28 dpi. cRNAs were labeled and hybridized to M430 2.0 chips according to Affymetrix protocols in

triplicate. Data were normalized with the Plier algorithm, Log transformed, and analyzed with GeneSpring GX 11.0 (Agilent Technologies Inc.). Significant genes were selected based on P values < 0.05 and fold change > 1.5 after correction for false discovery.

Real Time-PCR

Viral titers were determined by quantitation of viral RNA. RNA was prepared from whole lung homogenates using TRIzol (Sigma-Aldrich), and 2.5 μg of RNA was reverse transcribed into cDNA using random hexamer primers and Superscript II Reverse Transcriptase (Invitrogen). Quantitative PCR was performed to amplify the polymerase (PA) gene of A/PR8-OVA$_{II}$ using an ABI Prism 7700 Sequence Detector (Applied Biosystems) with 50 ng of cDNA per reaction and the following primers and probe: forward primer, 5′-CGGTCCAAATTCCTGCTGA-3′; reverse primer, 5′CATTGGGTTCCTTCCATCCA-3′; probe, 5′-6-FAM-CCAAGTCATGAAGGAGAGGGAATACCGCT-3′. Data were analyzed with Sequence Detector v1.7a (Applied Biosystems). The copy number of the PA gene per 50 ng of cDNA was calculated using a PA-containing plasmid of known concentration as a standard.

Statistical analysis

Unpaired, two-tailed, Students t-tests, $\propto = 0.05$, were used to assess whether the means of two normally distributed groups differed significantly. One-way ANOVA analysis with Bonferroni's multiple comparison post-test was employed to compare multiple means. All error bars represent the standard deviation. Significance is indicated as * $P < 0.05$, ** $P < 0.005$, *** $P < 0.001$, **** $P < 0.0001$.

Data availability

Microarray data that support the findings of this study will be deposited in the Gene Expression Omnibus with accession number XXX. (We will submit pending acceptance).

Supplementary Material

Refer to Web version on PubMed Central for supplementary material.

Acknowledgments

References

1. Swain SL, McKinstry KK, Strutt TM. Expanding roles for CD4(+) T cells in immunity to viruses. Nat Rev Immunol. 2012; 12(2):136–148. [PubMed: 22266691]

2. Mueller SN, Gebhardt T, Carbone FR, Heath WR. Memory T cell subsets, migration patterns, and tissue residence. Annu Rev Immunol. 2013; 31:137–161. [PubMed: 23215646]

3. Strutt TM, McKinstry KK, Marshall NB, Vong AM, Dutton RW, Swain SL. Multipronged CD4(+) T-cell effector and memory responses cooperate to provide potent immunity against respiratory virus. Immunol Rev. 2013; 255(1):149–164. [PubMed: 23947353]

4. Shin H, Iwasaki A. Tissue-resident memory T cells. Immunol Rev. 2013; 255(1):165–181. [PubMed: 23947354]

5. Bevan MJ. Memory T cells as an occupying force. Eur J Immunol. 2011; 41(5):1192–1195. [PubMed: 21469134]

6. Mueller SN, Mackay LK. Tissue-resident memory T cells: local specialists in immune defence. Nat Rev Immunol. 2015

7. Mackay LK, Rahimpour A, Ma JZ, Collins N, Stock AT, Hafon ML, et al. The developmental pathway for CD103(+)CD8+ tissue-resident memory T cells of skin. Nat Immunol. 2013; 14(12): 1294–1301. [PubMed: 24162776]

8. Laidlaw BJ, Zhang N, Marshall HD, Staron MM, Guan T, Hu Y, et al. CD4(+) T Cell Help Guides Formation of CD103(+) Lung-Resident Memory CD8(+) T Cells during Influenza Viral Infection. Immunity. 2014; 41(4):633–645. [PubMed: 25308332]

9. Casey KA, Fraser KA, Schenkel JM, Moran A, Abt MC, Beura LK, et al. Antigenindependent differentiation and maintenance of effector-like resident memory T cells in tissues. J Immunol. 2012; 188(10):4866–4875. [PubMed: 22504644]

10. Yu CI, Becker C, Wang Y, Marches F, Helft J, Leboeuf M, et al. Human CD1c+ dendritic cells drive the differentiation of CD103+ CD8+ mucosal effector T cells via the cytokine TGF-beta. Immunity. 2013; 38(4):818–830. [PubMed: 23562160]

11. Sheridan BS, Pham QM, Lee YT, Cauley LS, Puddington L, Lefrancois L. Oral infection drives a distinct population of intestinal resident memory CD8(+) T cells with enhanced protective function. Immunity. 2014; 40(5):747–757. [PubMed: 24792910]

12. El-Asady R, Yuan R, Liu K, Wang D, Gress RE, Lucas PJ, et al. TGF-{beta}-dependent CD103 expression by CD8(+) T cells promotes selective destruction of the host intestinal epithelium during graft-versus-host disease. J Exp Med. 2005; 201(10):1647–1657. [PubMed: 15897278]

13. Wakim LM, Smith J, Caminschi I, Lahoud MH, Villadangos JA. Antibody-targeted vaccination to lung dendritic cells generates tissue-resident memory CD8 T cells that are highly protective against influenza virus infection. Mucosal Immunol. 2015; 8(5):1060–1071. [PubMed: 25586557]

14. Turner DL, Farber DL. Mucosal resident memory CD4 T cells in protection and immunopathology. Front Immunol. 2014; 5:331. [PubMed: 25071787]

15. Sathaliyawala T, Kubota M, Yudanin N, Turner D, Camp P, Thome JJ, et al. Distribution and Compartmentalization of Human Circulating and Tissue-Resident Memory T Cell Subsets. Immunity. 2012

16. McKinstry KK, Strutt TM, Bautista B, Zhang W, Kuang Y, Cooper AM, et al. Effector CD4 T-cell transition to memory requires late cognate interactions that induce autocrine IL-2. Nat Commun. 2014; 5:5377. [PubMed: 25369785]

17. Bautista BL, Devarajan P, McKinstry KK, Strutt TM, Vong AM, Jones MC, et al. Short-Lived Antigen Recognition but Not Viral Infection at a Defined Checkpoint Programs Effector CD4 T Cells To Become Protective Memory. J Immunol. 2016; 197(10):3936–3949. [PubMed: 27798159]

18. Thomas PG, Brown SA, Yue W, So J, Webby RJ, Doherty PC. An unexpected antibody response to an engineered influenza virus modifies CD8+ T cell responses. Proc Natl Acad Sci U S A. 2006; 103(8):2764–2769. [PubMed: 16473934]

19. Anderson KG, Mayer-Barber K, Sung H, Beura L, James BR, Taylor JJ, et al. Intravascular staining for discrimination of vascular and tissue leukocytes. Nat Protoc. 2014; 9(1):209–222. [PubMed: 24385150]

20. Turner DL, Bickham KL, Thome JJ, Kim CY, D'Ovidio F, Wherry EJ, et al. Lung niches for the generation and maintenance of tissue-resident memory T cells. Mucosal Immunol. 2014; 7(3): 501–510. [PubMed: 24064670]

21. Wu T, Hu Y, Lee YT, Bouchard KR, Benechet A, Khanna K, et al. Lung-resident memory CD8 T cells (TRM) are indispensable for optimal cross-protection against pulmonary virus infection. J Leukoc Biol. 2014; 95(2):215–224. [PubMed: 24006506]

22. Park CO, Kupper TS. The emerging role of resident memory T cells in protective immunity and inflammatory disease. Nat Med. 2015; 21(7):688–697. [PubMed: 26121195]

23. Mackay LK, Braun A, Macleod BL, Collins N, Tebartz C, Bedoui S, et al. Cutting edge: CD69 interference with sphingosine-1-phosphate receptor function regulates peripheral T cell retention. J Immunol. 2015; 194(5):2059–2063. [PubMed: 25624457]

24. Skon CN, Lee JY, Anderson KG, Masopust D, Hogquist KA, Jameson SC. Transcriptional downregulation of S1pr1 is required for the establishment of resident memory CD8+ T cells. Nat Immunol. 2013; 14(12):1285–1293. [PubMed: 24162775]

25. Moran AE, Holzapfel KL, Xing Y, Cunningham NR, Maltzman JS, Punt J, et al. T cell receptor signal strength in Treg and iNKT cell development demonstrated by a novel fluorescent reporter mouse. J Exp Med. 2011; 208(6):1279–1289. [PubMed: 21606508]

26. Jelley-Gibbs DM, Brown DM, Dibble JP, Haynes L, Eaton SM, Swain SL. Unexpected prolonged presentation of influenza antigens promotes CD4 T cell memory generation. J Exp Med. 2005; 202(5):697–706. [PubMed: 16147980]

27. Kondrack RM, Harbertson J, Tan JT, McBreen ME, Surh CD, Bradley LM. Interleukin 7 regulates the survival and generation of memory CD4 cells. J Exp Med. 2003; 198(12):1797–1806. [PubMed: 14662907]

28. Brinkmann V, Davis MD, Heise CE, Albert R, Cottens S, Hof R, et al. The immune modulator FTY720 targets sphingosine 1-phosphate receptors. J Biol Chem. 2002; 277(24):21453–21457. [PubMed: 11967257]

29. Wakim LM, Woodward-Davis A, Liu R, Hu Y, Villadangos J, Smyth G, et al. The molecular signature of tissue resident memory CD8 T cells isolated from the brain. J Immunol. 2012; 189(7): 3462–3471. [PubMed: 22922816]

30. Hombrink P, Helbig C, Backer RA, Piet B, Oja AE, Stark R, et al. Programs for the persistence, vigilance and control of human CD8+ lung-resident memory T cells. Nat Immunol. 2016

31. McKinstry KK, Strutt TM, Kuang Y, Brown DM, Sell S, Dutton RW, et al. Memory CD4+ T cells protect against influenza through multiple synergizing mechanisms. J Clin Invest. 2012; 122(8): 2847–2856. [PubMed: 22820287]

32. Wakim LM, Woodward-Davis A, Bevan MJ. Memory T cells persisting within the brain after local infection show functional adaptations to their tissue of residence. Proc Natl Acad Sci U S A. 2010; 107(42):17872–17879. [PubMed: 20923878]

33. Strutt TM, McKinstry KK, Dibble JP, Winchell C, Kuang Y, Curtis JD, et al. Memory CD4+ T cells induce innate responses independently of pathogen. Nat Med. 2010; 16(5):558–564. 551–564. [PubMed: 20436484]

34. Chapman TJ, Lambert K, Topham DJ. Rapid reactivation of extralymphoid CD4 T cells during secondary infection. PLoS ONE. 2011; 6(5):e20493. [PubMed: 21647373]

35. Purton JF, Tan JT, Rubinstein MP, Kim DM, Sprent J, Surh CD. Antiviral CD4+ memory T cells are IL-15 dependent. J Exp Med. 2007; 204(4):951–961. [PubMed: 17420265]

36. Verbist KC, Cole CJ, Field MB, Klonowski KD. A role for IL-15 in the migration of effector CD8 T cells to the lung airways following influenza infection. J Immunol. 2011; 186(1):174–182. [PubMed: 21098221]

37. Yokoyama S, Watanabe N, Sato N, Perera PY, Filkoski L, Tanaka T, et al. Antibody-mediated blockade of IL-15 reverses the autoimmune intestinal damage in transgenic mice that overexpress IL-15 in enterocytes. Proc Natl Acad Sci U S A. 2009; 106(37):15849–15854. [PubMed: 19805228]

38. Richer MJ, Pewe LL, Hancox LS, Hartwig SM, Varga SM, Harty JT. Inflammatory IL-15 is required for optimal memory T cell responses. J Clin Invest. 2015; 125(9):3477–3490. [PubMed: 26241055]

39. Marcais A, Cherfils-Vicini J, Viant C, Degouve S, Viel S, Fenis A, et al. The metabolic checkpoint kinase mTOR is essential for IL-15 signaling during the development and activation of NK cells. Nat Immunol. 2014; 15(8):749–757. [PubMed: 24973821]

40. Nakamura R, Maeda N, Shibata K, Yamada H, Kase T, Yoshikai Y. Interleukin-15 is critical in the pathogenesis of influenza a virus-induced acute lung injury. J Virol. 2010; 84(11):5574–5582. [PubMed: 20335267]

41. Prlic M, Blazar BR, Farrar MA, Jameson SC. In vivo survival and homeostatic proliferation of natural killer cells. J Exp Med. 2003; 197(8):967–976. [PubMed: 12695488]

42. Hondowicz BD, An D, Schenkel JM, Kim KS, Steach HR, Krishnamurty AT, et al. Interleukin-2-Dependent Allergen-Specific Tissue-Resident Memory Cells Drive Asthma. Immunity. 2016; 44(1):155–166. [PubMed: 26750312]

43. Dooms H, Desmedt M, Vancaeneghem S, Rottiers P, Goossens V, Fiers W, et al. Quiescence-inducing and antiapoptotic activities of IL-15 enhance secondary CD4+ T cell responsiveness to antigen. J Immunol. 1998; 161(5):2141–2150. [PubMed: 9725205]

44. Ring AM, Lin JX, Feng D, Mitra S, Rickert M, Bowman GR, et al. Mechanistic and structural insight into the functional dichotomy between IL-2 and IL-15. Nat Immunol. 2012; 13(12):1187–1195. [PubMed: 23104097]

45. Zhang Q, Dove CG, Hor JL, Murdock HM, Strauss-Albee DM, Garcia JA, et al. DOCK8 regulates lymphocyte shape integrity for skin antiviral immunity. J Exp Med. 2014; 211(13):2549–2566. [PubMed: 25422492]

46. Zaid A, Hor JL, Christo SN, Groom JR, Heath WR, Mackay LK, et al. Chemokine Receptor-Dependent Control of Skin Tissue-Resident Memory T Cell Formation. J Immunol. 2017; 199(7): 2451–2459. [PubMed: 28855310]

47. Hombrink P, Helbig C, Backer RA, Piet B, Oja AE, Stark R, et al. Programs for the persistence, vigilance and control of human CD8+ lung-resident memory T cells. Nat Immunol. 2016; 17(12): 1467–1478. [PubMed: 27776108]

48. Teijaro JR, Verhoeven D, Page CA, Turner D, Farber DL. Memory CD4 T cells direct protective responses to influenza virus in the lungs through helper-independent mechanisms. J Virol. 2010; 84(18):9217–9226. [PubMed: 20592069]

49. Olson MR, Seah SG, Cullen J, Greyer M, Edenborough K, Doherty PC, et al. Helping Themselves: Optimal Virus-Specific CD4 T Cell Responses Require Help via CD4 T Cell Licensing of Dendritic Cells. J Immunol. 2014; 193(11):5420–5433. [PubMed: 25339661]

50. Chu C, Wang Y, Zhang X, Ni X, Cao J, Xu W, et al. SAP-regulated T Cell-APC adhesion and ligation-dependent and -independent Ly108-CD3zeta interactions. J Immunol. 2014; 193(8):3860–3871. [PubMed: 25217164]

51. Josien R, Wong BR, Li HL, Steinman RM, Choi Y. TRANCE, a TNF family member, is differentially expressed on T cell subsets and induces cytokine production in dendritic cells. J Immunol. 1999; 162(5):2562–2568. [PubMed: 10072496]

52. Josien R, Li HL, Ingulli E, Sarma S, Wong BR, Vologodskaia M, et al. TRANCE, a tumor necrosis factor family member, enhances the longevity and adjuvant properties of dendritic cells in vivo. J Exp Med. 2000; 191(3):495–502. [PubMed: 10662795]

53. Jabri B, Abadie V. IL-15 functions as a danger signal to regulate tissue-resident T cells and tissue destruction. Nat Rev Immunol. 2015; 15(12):771–783. [PubMed: 26567920]

54. Valkenburg SA, Li OT, Mak PW, Mok CK, Nicholls JM, Guan Y, et al. IL-15 adjuvanted multivalent vaccinia-based universal influenza vaccine requires CD4+ T cells for heterosubtypic protection. Proc Natl Acad Sci U S A. 2014; 111(15):5676–5681. [PubMed: 24706798]
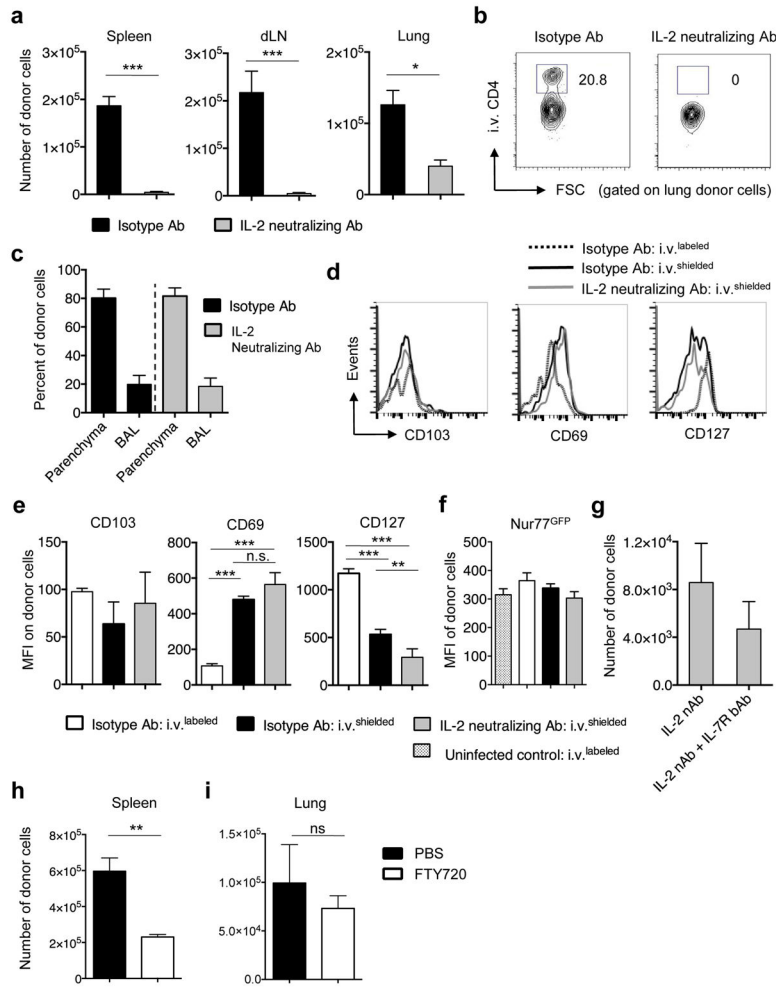
Figure 1.
A T$_{RM}$-associated phenotype is expressed by i.v.^{shielded} lung memory cells. Unprimed B6 mice received 1×10^6 congenic donor cells followed by priming with IAV and treatment from 1–7 dpi with IL-2 neutralizing Abs or isotype control Ab. (a) Donor cells were enumerated at 28 dpi in stated organs (4 mice/group; one of 3 similar experiments). (b) At 28 dpi, recipient mice were injected i.v. with fluorescent Ab specific for CD4 and the frequency of donor cells stained (i.v.^{labeled}) or not (i.v.^{shielded}) was determined (representative staining). (c) The percentage of donor cells at 28 dpi recovered either in the BAL or from the lung parenchyma (3 mice/group; one of 2 experiments). Representative staining (d) and mean fluoresce intensity (MFI) analysis (e) for donor cell for CD103, CD69, and CD127. (f) Nur77^{GFP} OT-II donors were analyzed for GFP expression at 28 dpi discriminated based on their ability to be labeled by i.v. administered CD4 Ab (3 mice per group; one of 2 experiments). (g) Mice receiving donor cells were treated with IL-2 neutralizing Ab (IL-2n Ab) from 1–7 dpi, followed by treatment with PBS or with IL-7 receptor blocking Ab every other day from 10–26 dpi. The number of donor cells recovered from the lungs at 28 dpi is shown (4 mice per group; one of two experiments). Mice receiving donor cells and IAV priming were treated or not with FTY720 for 5 consecutive days beginning on 23 dpi. On 28
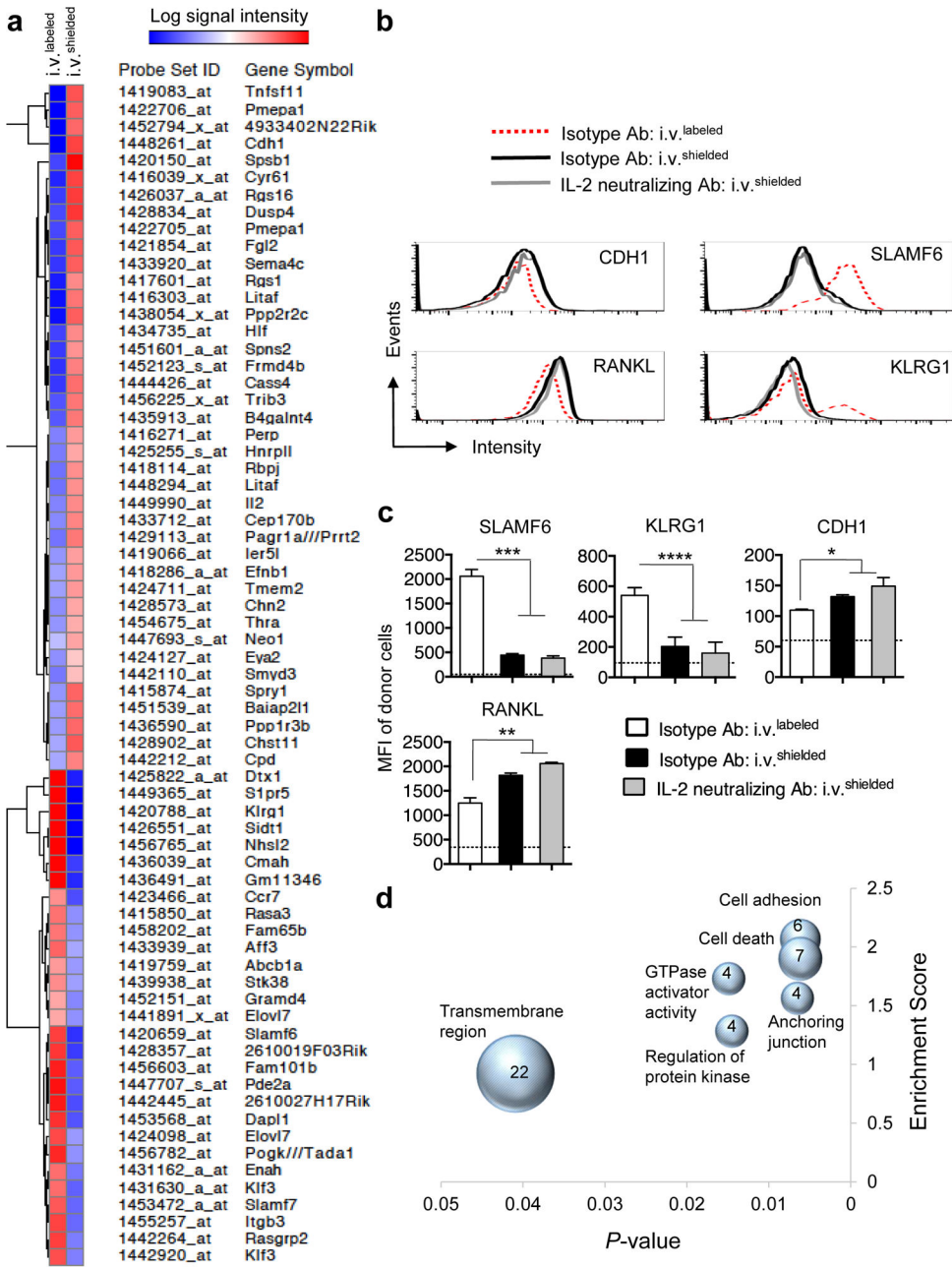
dpi (h) spleens and (i) lungs were analyzed for total donor cells (3 mice per group; one of two experiments).

Figure 2.

CD4 T_{RM} express a unique transcriptional signature. OT-II cells were sort-purified from IAV-primed hosts at 28 dpi. Whole genome microarray was performed comparing i.v.^{shielded} lung donor cells to i.v.^{labeled} donor cells obtained from the lung and spleen. (a) Summary of genes differentially expressed by i.v.^{shielded} and i.v.^{labeled} donor cells at a threshold of > 1.5-fold and *P* value of 0.05. (b) Representative staining of validation of differential surface marker expression from stated subsets and (c) MFI analysis from 3 mice per group (dotted line in bar graphs represent FMO control staining for each marker; one of 3 independent experiments). (d) DAVID functional annotation analysis was performed on the genes summarized in Supplemental Table I that were differentially expressed by i.v.^{shielded} and
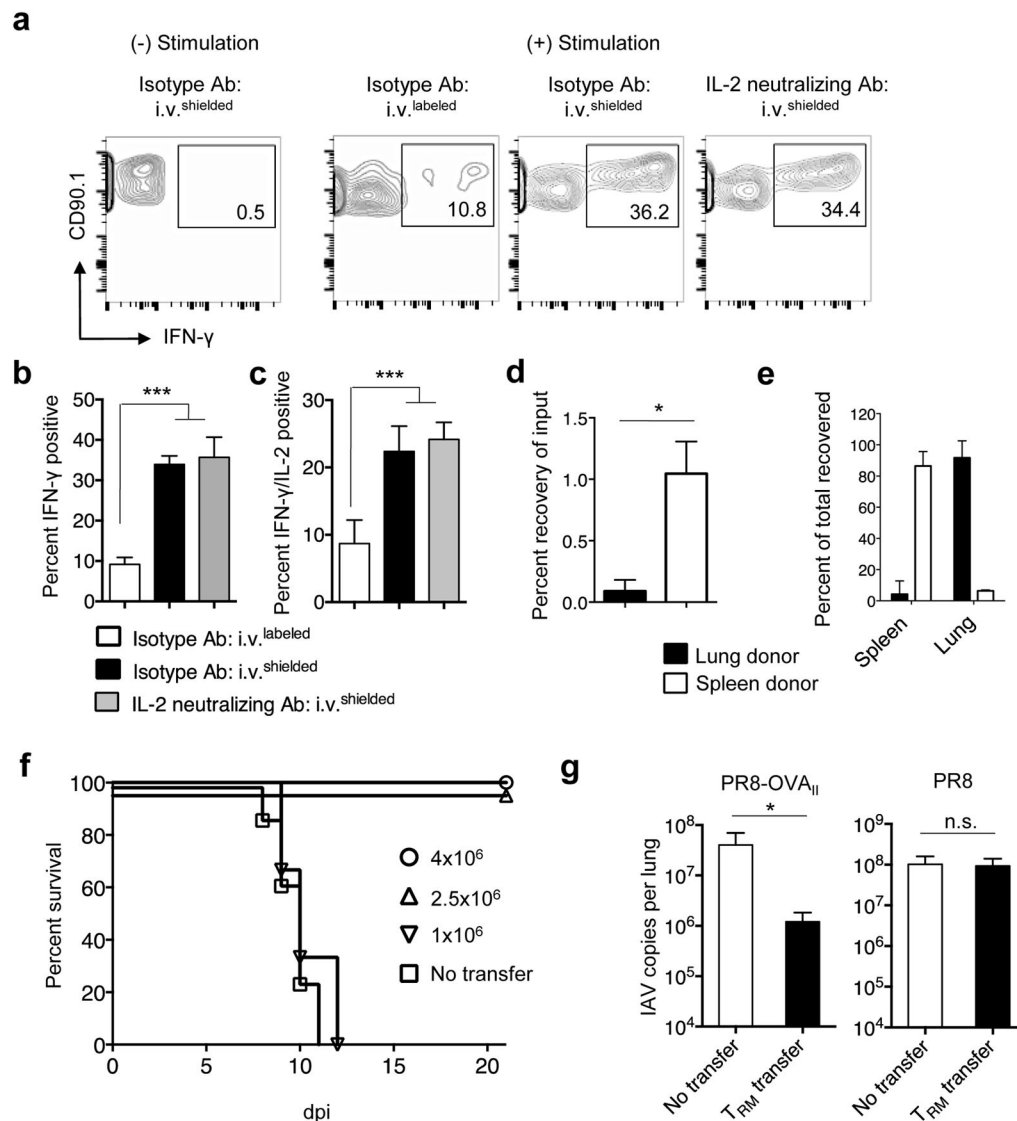
i.v.^{labeled} donor cells. The most significantly enriched pathways (*P* value of 0.05) as well as the number of genes in each pathway are shown.

Figure 3.

CD4 T_{RM} display enhanced cytokine production capacity versus conventional memory cells. At 28 dpi, donor cells in the lungs of IAV-primed mice were assessed for their ability to produce cytokines based on labeling with i.v. administered fluorescent CD4 Ab. (a) Representative staining of unstimulated (upper row) or stimulated i.v.^{labeled} and i.v.^{shielded} donor cells (gated on Thy1.1$^+$ cells) for IFN-γ and summary of the frequency of (b) IFNγ-producing and (c) dual IFN-γ and IL-2-producing donor cells from 3 mice per group (one of 3 experiments). An equal number of donor T_{RM} or splenic i.v.^{labeled} donor cells sort-purified from IAV-primed mice were transferred i.v. to new hosts in the absence of IAV infection. After 7 days, the total number of donor cells recovered from the spleen and lungs of adoptive hosts was determined. Shown is (d) the percentage of either donor population recovered relative to input, and (e) the percentage of total donor cells recovered from either spleens or lungs of adoptive hosts (4 mice per group). Donor T_{RM} isolated from IAV-primed mice and 5×10^6, 2.5×10^6, or 1×10^6 were transferred i.n. to unprimed mice followed by
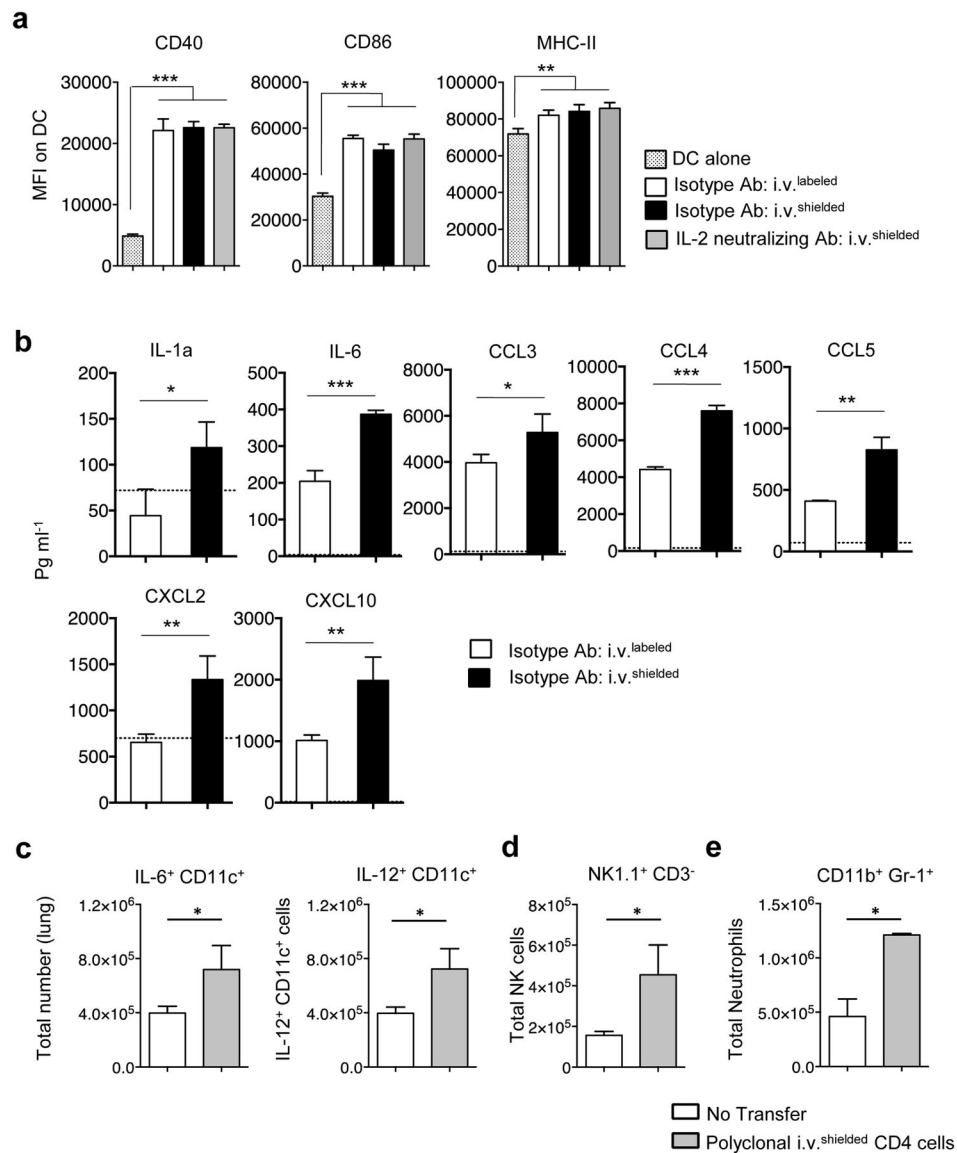
challenge with a lethal dose of PR8-OVA$_{II}$. (f) Survival of mice receiving T$_{RM}$ versus no transfer controls is shown (combined results from 3 separate experiments with 3 mice/ group). (g) The viral titer from mice receiving 2.5×10^6 donor (OT-II) T$_{RM}$ or not and challenged with either PR8-OVA$_{II}$ (left) or PR8 (right) (3–4 mice per group).

Figure 4.

Lung T_{RM} induce a more rapid inflammatory response from dendritic cells than conventional memory CD4 T cells. Donor memory cells, 1×10^5, sort-purified from the lungs or spleens of IAV-primed mice on the basis of their ability to be labeled by CD4 Ab administered i.v. were cultured with an equal number of bone marrow-derived DC pulsed with OVA$_{II}$ peptide. (a) After 40 hours, DC were analyzed for expression of molecules associated with their activation by FACS (triplicate conditions; one of two experiments). (b) Supernatants from cultures of DC and memory cells were harvested at 40 hours and analyzed for stated cytokines and chemokines by luminex. Dotted lines indicate the average level detected in supernatants from wells containing DC and peptide alone (triplicate conditions; one of two experiments). Sort-purified polyclonal i.v.^{shielded} CD4 T cells from the lungs of IAV-primed mice were transferred to unprimed mice followed by PR8 challenge. At 4 dpi, lungs were harvested and analyzed for the presence of (c) IL-6$^+$ and
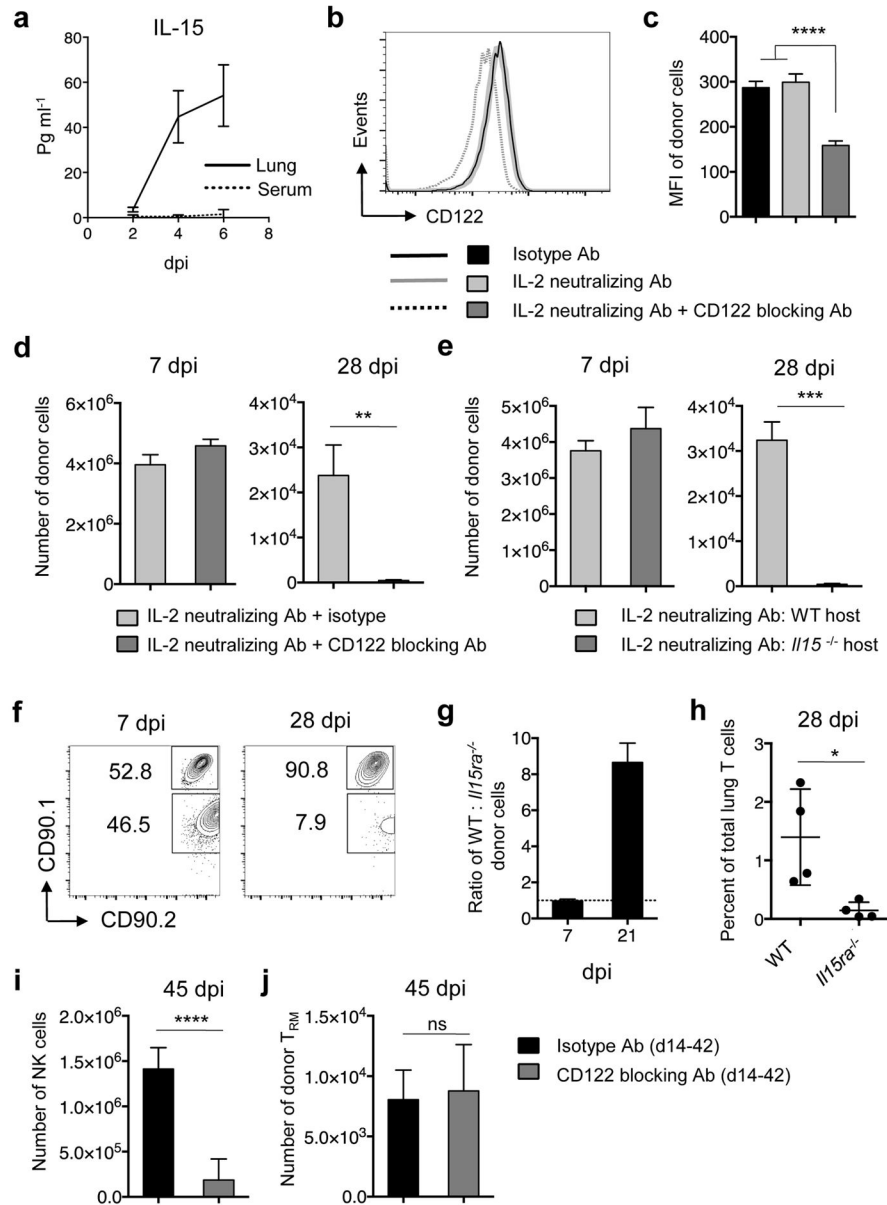
IL-12$^+$ CD11c$^+$ cells, (d) NK cells, and (e) neutrophils and compared to mice not receiving donor cells (3–4 mice/group; 1 of 2 experiments).

Figure 5.
IL-15 is required for the generation of lung CD4 T$_{RM}$. (a) Lung homogenate and serum was analyzed from IAV-primed mice on stated days for presence of IL-15 protein (4 mice/group; one of 4 experiments). Mice receiving donor cells and IAV priming were treated either with IL-2 neutralizing Ab alone, or with IL-2 neutralizing Ab and CD122 blocking Abs from 1–7 dpi. (b and c) On 7 dpi, donor cells in the lungs were analyzed for expression of CD122 (representative from 1 of 4 mice; 1 of 3 similar experiments). (d) The number of donor cells present in the lung at 7 dpi and 28 dpi in mice treated as in (A) is shown (4 mice per group). Donor cells were transferred to either WT or *Il15*$^{-/-}$ hosts that were then primed with IAV and treated with IL-2 neutralizing Ab from 1–7 dpi. (e) Donor cells in the lung were enumerated at 7 and 28 dpi (3 mice per group; 1 of 3 experiments). WT (Thy1.1/Thy1.2) and *Il15ra*$^{-/-}$ OT-II cells (Thy1.2) were transferred to WT CD45.1$^+$ hosts that were primed

with IAV and treated with IL-2 neutralizing Ab. (f) Representative staining for both donor populations at 7 and 28 dpi and (g) the ratio of WT: *Il15ra*$^{-/-}$ donor cells detected when co-transferred at 7 and 28 dpi and (h) the recovery of WT versus *Il15ra*$^{-/-}$ donor cells when transferred to seperate hosts at 28 dpi (4 mice/group; one of two experiments). Mice receiving WT donor cells and challenged with IAV were treated with IL-2 neutralizing Abs from 1–7 dpi, and with CD122 blocking Ab or an isotype control every second day from 14 to 44 dpi. (i) The number of NK cells recovered from the spleens of mice at and (j) the number of donor T$_{RM}$ recovered from the lung at 45 dpi was determined from 4 mice/group (1 of 2 experiments).

Table I

Genes differentially expressed by lung CD4+ T_{RM} generated by IAV challenge and published CD103$^+$ CD8$^+$ T_{RM} from various models and tissues

Gene	Product	↑/↓ T_{RM}	Ref
Cdh1	Cadherin 1	↑ in T_{RM}	1,2
Chn2	Chimerin 2	↑ in T_{RM}	1
Litaf	Lipopolysaccharide-induced tumor-necrosis factor	↑ in T_{RM}	1,2
Rgs1	Regulator of G-protein signaling 1	↑ in T_{RM}	1
Rgs16	Regulator of G-protein signaling 16	↑ in T_{RM}	2
Cmah	Cytidine monophospho-N-acetylneuraminic acide hydroxylase	↓ in T_{RM}	1
Elovl7	ELOVL family member 7, elongation of long chain fatty acids	↓ in T_{RM}	1
Fam65b	Family with sequence similarity 65, member B	↓ in T_{RM}	1
Rasgrp2	RAS, guanyl releasing protein 2	↓ in T_{RM}	1
S1pr5	Shingosine 1-phosphate receptor 5	↓ in T_{RM}	1
Sidt1	SID1 transmembrane family, member 1	↓ in T_{RM}	1,2
Slamf6	SLAM family member 6	↓ in T_{RM}	1,2
Klf3	Krueppel-like factor 3	↓ in T_{RM}	2
Aff3	AF4/FMR2 family member 3	↓ in T_{RM}	2
Ccr7	C-C chemokine receptor type 7	↓ in T_{RM}	2
Dtx1	Protein deltex-1	↓ in T_{RM}	2